

IDENTIFICATION OF THE AMORPHOUS PHASE IN PLASMA SPRAYED APATITE COATINGS

K. A. Gross^{1,2}, M. Phillips², B. Ben-Nissan³, C. C. Berndt⁴

¹Department of Materials Engineering, Monash University, Clayton 3168, Australia.

²Microstructural Analysis Unit, University of Technology, Sydney, Australia; ³Department of Chemistry, Materials and Forensic Sciences, University of Technology, Sydney, Australia;

⁴Department of Materials Science and Engineering, SUNY at Stony Brook, USA.

ABSTRACT

Most hydroxyapatite coated implants produced by plasma spraying contain the amorphous phase which affects the longevity of the coatings. It is thus necessary to measure, locate and quantify this in the microstructure for quality control and analysis of retrieved implants. Several methods are available both for micro-characterization and analysis on the calcium phosphate coatings. These techniques include microscopy (optical, secondary electron and cathodoluminescence), spectroscopy (infra-red and Raman), thermal analysis and X-ray diffraction. The amorphous phase produces peak broadening in infra-red, however the interpretation is complex due to the contribution of residual stresses. Raman spectroscopy yields an individual peak located at 950 cm^{-1} . Crystallization events in thermal analysis indicate that the chemical composition of the amorphous phase may be hydroxyl rich or hydroxyl depleted. The most useful of these techniques is microscopy where the location, distribution, size and quantity of these regions can be readily ascertained. The information from these techniques will be discussed to reveal the nature and facilitate identification of the amorphous phase.

KEYWORDS: amorphous, characterization, microstructure, hydroxyapatite, plasma spraying

INTRODUCTION

Crystallinity is an important parameter to measure insofar that it influences the degradation of hydroxyapatite coatings and hence the stabilization of dental and orthopaedic biomedical devices. In the past, crystallinity has been defined as a measure of crystal size and/or lattice perfection in reference to chemically synthesized homogeneous powders or the inorganic fraction of bone.¹ The measurement was mainly performed with X-ray diffraction and supplemented with infra-red spectroscopy. A lower crystallinity material was described by a lower diffraction peak intensity with respect to the background in X-ray diffraction patterns or a loss of resolution of the various vibrational modes in the PO_4 bands in infra-red spectra.²

Crystallinity in reference to coatings, produced by plasma spraying hydroxyapatite, includes both the lower crystal perfection caused by cooling from high temperatures and an amorphous phase, which like a glass, has no long range order. The adopted definition of crystallinity in plasma sprayed coatings refers to the amount of amorphous phase present in the

coatings. Characteristics of the amorphous and the crystalline phase will be identified to enable macro or micro characterization of the coatings.

METHODS

Coatings used for analysis include those produced at The Thermal Spray Laboratory, State University of New York at Stony Brook and a commercially available coating.

Powder was prepared for thermal analysis, infra-red spectroscopy, and X-ray diffraction by crushing in a mortar and pestle. The coating otherwise was polished to a surface finish of $0.05\mu\text{m}$ for identification of amorphous regions with Raman spectroscopy or microscopy.

X-ray diffraction was conducted with Cu K α radiation over a two theta range of 20 to 40 degrees using a step size of 0.02 degrees and an acquisition time of 4 seconds per step.

Transparent tablets were produced by compressing a homogeneous mixture of the prepared powder with 1 wt.% KBr. This tablet was then subjected to infra-red spectroscopy analysis set to a resolution of 4 cm^{-1} .

Heat exchange was monitored upon heating at a rate of $10^{\circ}\text{C}/\text{min}$ with differential thermal analysis in a stagnant air atmosphere.

Laser-Raman microanalyses were conducted using the argon green line at 514.5 nm, with a laser power of 20 mW; exciting wavelength of 514.532 nm. A spectral slit width of 3.12 cm^{-1} was selected. Spectra from the irradiated area, using a spot diameter of $1\mu\text{m}^2$, were recorded within the range of 800 and 1200 cm^{-1} with an acquisition time of 200 seconds:

Cathodoluminescence (CL) microanalysis was performed using an Oxford Instruments MonoCL2 CL system attached to a JEOL 35C SEM equipped with a Microspec Wavelength Dispersive X-ray Spectrometer. Panchromatic CL images were collected using a Link ISIS digital image capture system at 1024×800 pixels with a 100 psec dwell time per pixel.

RESULTS AND DISCUSSION

X-ray diffraction of a plasma sprayed coatings with a medium crystallinity exhibited a decrease in diffraction peak intensity (Fig. 1). Hydroxyapatite is identified by the main peak intensity at 31.8° whereas the amorphous phase is detected by a broad peak centred at $30\text{-}31^{\circ}$.

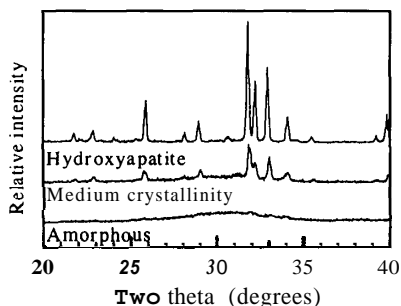


Figure 1. X-ray diffraction of an amorphous phase, medium crystallinity coating and hydroxyapatite.

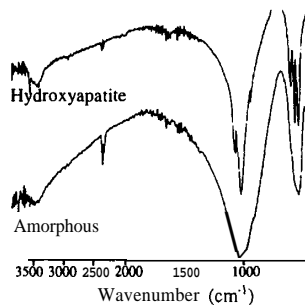


Figure 2. Infra-red spectra of an amorphous phase and hydroxyapatite.

This broad emission has been detected in other synthetic amorphous calcium phosphates with different compositions³ and is representative of a short range repetitive unit such as the bond length between the oxygen and the phosphorus in the phosphate groups. Similarly, infra-red spectra of the amorphous phase contains broad emission bands representing a wide variation of vibrations possible in the more unrestricted volume within the amorphous phase (Fig. 2). The broad emission represents contribution both from the stressed lattice and the amorphous phase.

While it is possible to distinguish different calcium phosphate phases with X-ray diffraction in their crystalline form, the differences in the short range order are very minimal. Energy X-ray absorption fine structure experiments conducted on acidic and basic calcium phosphates in the amorphous state have revealed very similar spectra.⁴

Raman microprobe on the crystalline and the amorphous areas within the coating produced peaks centred at 958 cm^{-1} and 950 cm^{-1} respectively (Fig. 3). This is in agreement with previously conducted work.⁷ The shift in the **Raman** band and the high intensity signal suggests that the components of residual stress and amorphous phase content would be easier to differentiate. Since tricalcium phosphate also exhibits a peak at 950 cm^{-1} , X-ray diffraction must be used in conjunction with **Raman** spectroscopy.

Differential thermal analysis (DTA) of hydroxyapatite (**HAp**) and the amorphous phase are similar except for a crystallization peak at 500 and $700\text{ }^{\circ}\text{C}$ (Fig. 4). These peaks suggest that the amorphous phase does not represent fine crystallites but a random positioning of the phosphate groups and calcium ions which after a rearrangement are able to form a stable hydroxyapatite. The two exothermic peaks are indicative of crystallization of a hydroxyl rich amorphous phase to hydroxyapatite at about $500\text{ }^{\circ}\text{C}$ and crystallization of a hydroxyl deficient amorphous phase to oxyapatite (**OAp**) at $720\text{ }^{\circ}\text{C}$.⁵ Plasma sprayed coatings containing the amorphous phase can thus contain localized areas with different hydroxyl ion concentrations.

Plasma sprayed coatings involve heat transfer through the coating which can promote the formation of small crystals. Identification of the amorphous phase by microscopy can lead to different interpretations of an amorphous phase. At the light microscopy magnification level, it is possible to distinguish the two areas based on the higher reflected light intensity from the crystalline phase (Fig. 5a). The amorphous phase (darker grey) is nonuniformly distributed within the coating and located around crystalline areas and adjacent to the substrate.⁶

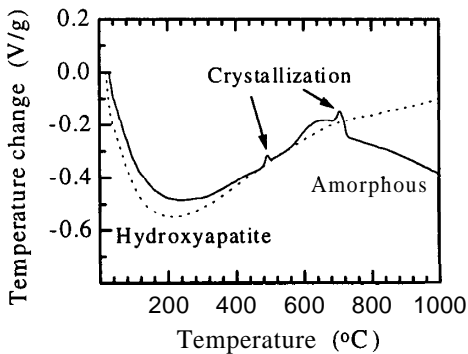


Figure 3. DTA of an amorphous phase and hydroxyapatite. Crystallization products are HAp at 500 and OAp at $720\text{ }^{\circ}\text{C}$.

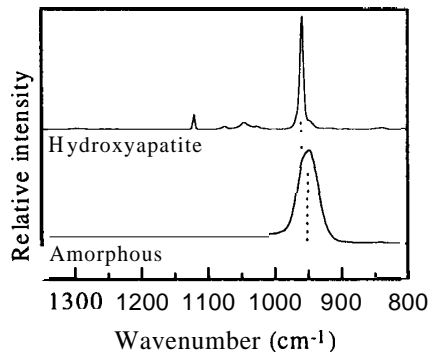


Figure 4. **Raman** spectra of an amorphous phase exhibits a broad phosphate band.

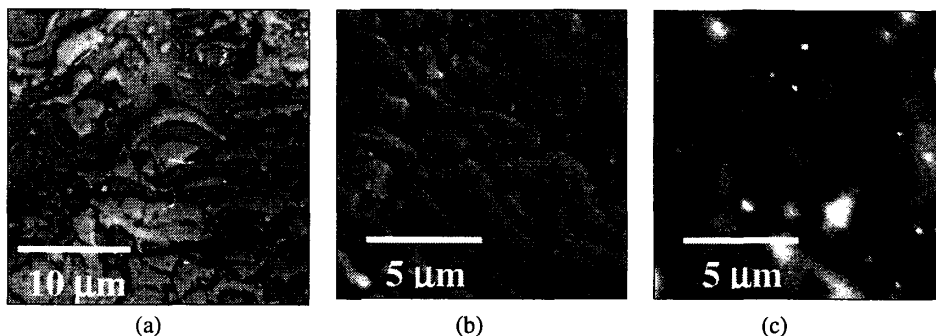


Figure 5. Microstructures of hydroxyapatite coatings in cross section as observed by (a) optical microscopy, (b) scanning electron microscopy and (c) cathodoluminescence microscopy. The lighter areas in (a) and (b) represent the crystalline phase and in (c) represent the amorphous regions. Field of view in (a) is 25 x 25 μm and in (b) and (c) is 12 x 12 μm .

Crystalline regions in a secondary electron image also appear lighter (Fig. 5b). The difference in intensity between the crystalline and the amorphous phase is lower than in light microscopy. The coating microstructure clearly shows long crystalline lamellae surrounded by the amorphous phase in a 70 wt.% crystallinity coating.

Cathodoluminescence microscopy uses the different light emission of the two phases during exposure to an electron beam. The light response from the amorphous phase is significantly higher than the crystalline phase. This allows a map to be made of the amorphous regions (Fig. 5c). Since the light is also emitted by subsurface amorphous areas, the cathodoluminescence image may not correspond exactly with the secondary electron image.

Cathodoluminescence microscopy can be performed on an unprepared flat surface like a histological section. This tool offers a means of detecting the amorphous phase not possible previously.

CONCLUSION

To completely identify the amorphous phase it is important to use several techniques. It is recommended that differential thermal analysis be used in conjunction with X-ray diffraction and light spectroscopy (either infra-red or **Raman**). Microscopy can then be used to identify the location of the amorphous phase within the microstructure of the coating.

ACKNOWLEDGEMENT

One of the authors (CCB) acknowledges support from NSF-MRSEC DMR9632570.

REFERENCES

1. Le Geros RZ. *Prog Crystal Growth Charact* 1981; 4:1-45.
2. Le Geros RZ, Shirra WP, Miravite MA, Le Geros JP. *Coll Int CNRS* 1973,230:105-115.
3. Posner AS, Betts F. *Accts Chem Res* 1975, **8**:273-281.
4. Nelson LS, Holt C, Harries JE, Hukins DWL. *Physica B*, 1989, **158(1-3)**: 105-6.
5. Gross KA, Gross V, Berndt CC. *J Amer Cer Soc* 1998, **81(1)**:106-12.
6. Gross KA, Berndt CC *et al. Int J Oral Maxillofac Implants*, 1997, **12**:589-597.
7. Weinlaender M, Beumer J, Kenney EB *et al. J Mater Sci: Mater in Med* 1992, **3**:397-401.